Jet production in deep inelastic ep scattering at HERA*

C. Glasman†
Universidad Autónoma de Madrid, Spain

Abstract

Recent results from jet production in deep inelastic ep scattering at HERA are reviewed. The values of $\alpha_s(M_Z)$ extracted from a QCD analysis of the data are presented.

1 Introduction

Jet production in neutral-current (NC) deep inelastic ep scattering (DIS) provides a test of perturbative QCD (pQCD) calculations and of the parametrisations of the proton parton densities (PDFs). Jet cross sections allow the determination of the fundamental parameter of QCD, the strong coupling constant α_s, and help to constrain the parton densities in the proton.

Up to leading order (LO) in α_s, jet production in NC DIS proceeds via the quark-parton model (QPM) ($Vq \to q$, where $V = \gamma$ or Z^0), boson-gluon fusion (BGF) ($Vg \to q\bar{q}$) and QCD-Compton (QCDC) ($Vq \to qg$) processes. The jet production cross section is given in pQCD by the convolution of the proton PDFs and the subprocess cross section,

$$d\sigma_{\text{jet}} = \sum_{a=q,\bar{q},g} \int dx \; f_a(x,\mu_F) \; d\hat{\sigma}_a(x,\alpha_s(\mu_R),\mu_R,\mu_F),$$

where x is the fraction of the proton's momentum taken by the interacting parton, f_a are the proton PDFs, μ_F is the factorisation scale, $\hat{\sigma}_a$ is the subprocess cross section and μ_R is the renormalisation scale.

All the data accumulated from HERA and fixed-target experiments have allowed a good determination of the proton PDFs over a large phase space. Then, measurements of jet production in neutral current DIS provide accurate tests of pQCD and a determination of the fundamental parameter of the theory, α_s.

At high scales, calculations using the DGLAP evolution equations have been found to give a good description of the data up to next-to-leading order (NLO). Therefore, by fitting the data with these calculations, it is possible to extract accurate values of α_s and the gluon density of the proton. However, for scales of $E_T^{\text{jet}} \sim Q$, where E_T^{jet} is the jet transverse energy and Q is the exchanged photon virtuality, and large values of the jet pseudorapidity, η^{jet}, large discrepancies between the data and the NLO calculations have been observed at low x. This could indicate

*Talk given at the "Ringberg workshop: New trends in HERA Physics 2003", Ringberg Castle, Germany, 28$^{\text{th}}$ September - 3$^{\text{rd}}$ October, 2003.

†Ramón y Cajal Fellow.

a breakdown of the DGLAP evolution and the onset of BFKL effects. These discrepancies can also be explained by assigning a partonic structure to the exchanged virtual photon or a large contribution of higher order effects at low Q^2.

2 Inclusive jet cross sections

Inclusive jet cross sections have been measured [1] in the Breit frame using the k_T-cluster algorithm in the longitudinally invariant mode. The measurements were made in the kinematic region given by $Q^2 > 125$ GeV^2 and $-0.7 < \cos\gamma < 0.5$, where γ is the angle of the struck quark in the quark-parton model in the HERA laboratory frame. The cross sections refer to jets of $E_{T,\mathrm{B}}^{\mathrm{jet}} > 8$ GeV and $-2 < \eta_{\mathrm{B}}^{\mathrm{jet}} < 1.8$, where $E_{T,\mathrm{B}}^{\mathrm{jet}}$ and $\eta_{\mathrm{B}}^{\mathrm{jet}}$ are the jet transverse energy and pseudorapidity, respectively, in the Breit frame.

The use of inclusive jet cross sections in a QCD analysis presents several advantages: inclusive jet cross sections are infrared insensitive and better suited to test resummed calculations and the theoretical uncertainties are smaller than for dijet cross sections.

Figure 1 shows the inclusive jet cross section as a function of Q^2 and $E_{T,\mathrm{B}}^{\mathrm{jet}}$. The dots are the data and the error bars represent the statistical and systematic uncertainties; the shaded band displays the uncertainty on the absolute energy scale of the jets. The measured cross sections have a steep fall-off, by five (four) orders of magnitude within the measured Q^2 ($E_{T,\mathrm{B}}^{\mathrm{jet}}$) range. The lines are the NLO calculations using DISENT with different choices of the renormalisation scale ($\mu_R = Q$ or $E_{T,\mathrm{B}}^{\mathrm{jet}}$). The calculations describe reasonably well the Q^2 and $E_{T,\mathrm{B}}^{\mathrm{jet}}$ dependence of the cross section for $Q^2 > 500$ GeV^2 and $E_{T,\mathrm{B}}^{\mathrm{jet}} > 15$ GeV. At low Q^2 and low $E_{T,\mathrm{B}}^{\mathrm{jet}}$, the measurements are above the calculations by about 10%, which is of the same size as the theoretical uncertainties (see below). Therefore, for the extraction of α_s, the phase space was restricted to high Q^2 and high $E_{T,\mathrm{B}}^{\mathrm{jet}}$.

The experimental uncorrelated uncertainties for these cross sections are small, $\sim 5\%$. The uncertainty coming from the absolute energy scale of the jets is also small, $\sim 5\%$. The theoretical uncertainties comprise 5% from the absent higher orders, 3% from the uncertainties of the proton PDFs and 5% from the uncertainty in the value of $\alpha_s(M_Z)$ assumed. The parton-to-hadron corrections are 10% with an uncertainty of 1%.

2.1 Determination of α_s

The method [1] used by ZEUS to extract α_s exploits the dependence of the NLO calculations on $\alpha_s(M_Z)$ through the matrix elements ($\hat{\sigma} \sim A \cdot \alpha_s + B \cdot \alpha_s^2$) and the proton PDFs ($\alpha_s(M_Z)$ value assumed in the evolution). To take into account properly this correlation, NLO calculations were performed using various sets of PDFs which assumed different values of $\alpha_s(M_Z)$. The calculations were then parametrised as a function of $\alpha_s(M_Z)$ in each measured Q^2 or $E_{T,\mathrm{B}}^{\mathrm{jet}}$ region. From the measured value of the cross section as a function of Q^2 in each region of Q^2, a value of $\alpha_s(M_Z)$ and its uncertainty were extracted using the parametrisations of the NLO calculations.

From the inclusive jet cross section for $Q^2 > 500$ GeV^2, the value

$$\alpha_s(M_Z) = 0.1212 \pm 0.0017\ (\mathrm{stat.})\ ^{+0.0023}_{-0.0031}\ (\mathrm{exp.})\ ^{+0.0028}_{-0.0027}\ (\mathrm{th.})$$

was extracted using the method explained above. The experimental uncertainties are dominated by the uncertainty on the absolute energy scale of the jets (1%). The theoretical uncertainties

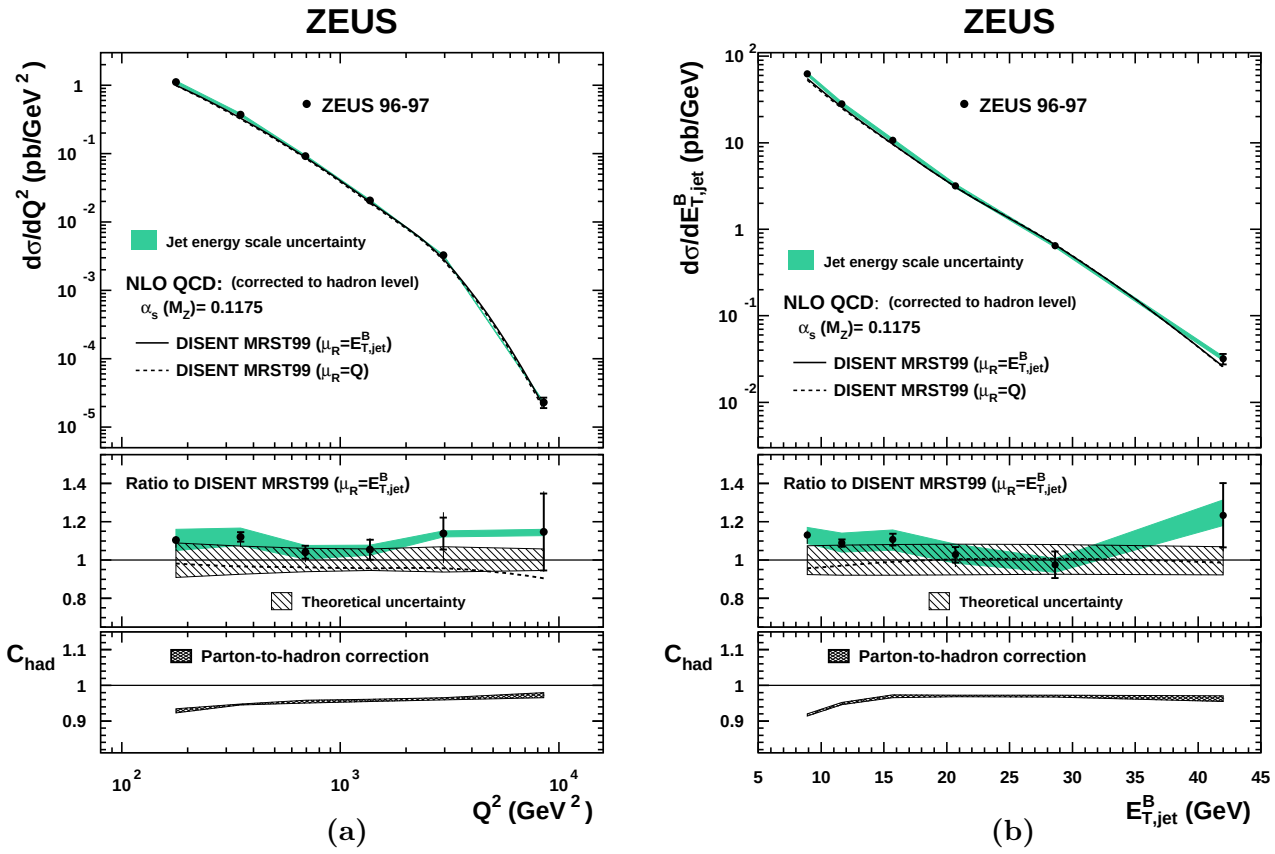

Figure 1: Inclusive jet cross sections [1] as a function of (a) Q^2 and (b) $E^{\rm jet}_{T,\rm B}$.

are: 3% from the absent higher orders, 1% from the PDFs and 0.2% from the hadronisation corrections. This determination is compatible with other independent extractions performed at HERA and with the current world average (see figure 2a). Further precision in the extraction of $\alpha_s(M_Z)$ from inclusive jet cross sections depends upon further experimental and theoretical improvements.

The QCD prediction for the energy-scale dependence of α_s has been tested by determining α_s from the measured differential cross sections at different scales [1]. From the measured cross section as a function of $E^{\rm jet}_{T,\rm B}$, in each region of $E^{\rm jet}_{T,\rm B}$, a value of $\alpha_s(E^{\rm jet}_{T,\rm B})$ was extracted. The result, shown in figure 2b (triangles), is compatible with the running of α_s as predicted by QCD (shaded band) over a large range in the scale. Figure 2b also shows other studies of the energy-scale dependence of α_s from HERA: all the results are compatible with each other and with the QCD prediction. This constitutes a test of the scale dependence of α_s between $\mu = 8.4$ and 90 GeV.

3 Parton evolution at low x

Dijet data in DIS may be used to gain insight into the parton dynamics at low x. The evolution of the PDFs with the factorisation scale can be described by the DGLAP evolution equations which sum the leading powers of terms like $\alpha_s \log Q^2$ in the region of strongly ordered transverse momenta k_T. This presciption describes successfully jet production at high Q^2. However, the DGLAP approximation is expected to break down at low x since when $\log Q^2 \ll \log 1/x$, the terms proportional to $\alpha_s \log 1/x$ become important and need to be summed. This is done in the

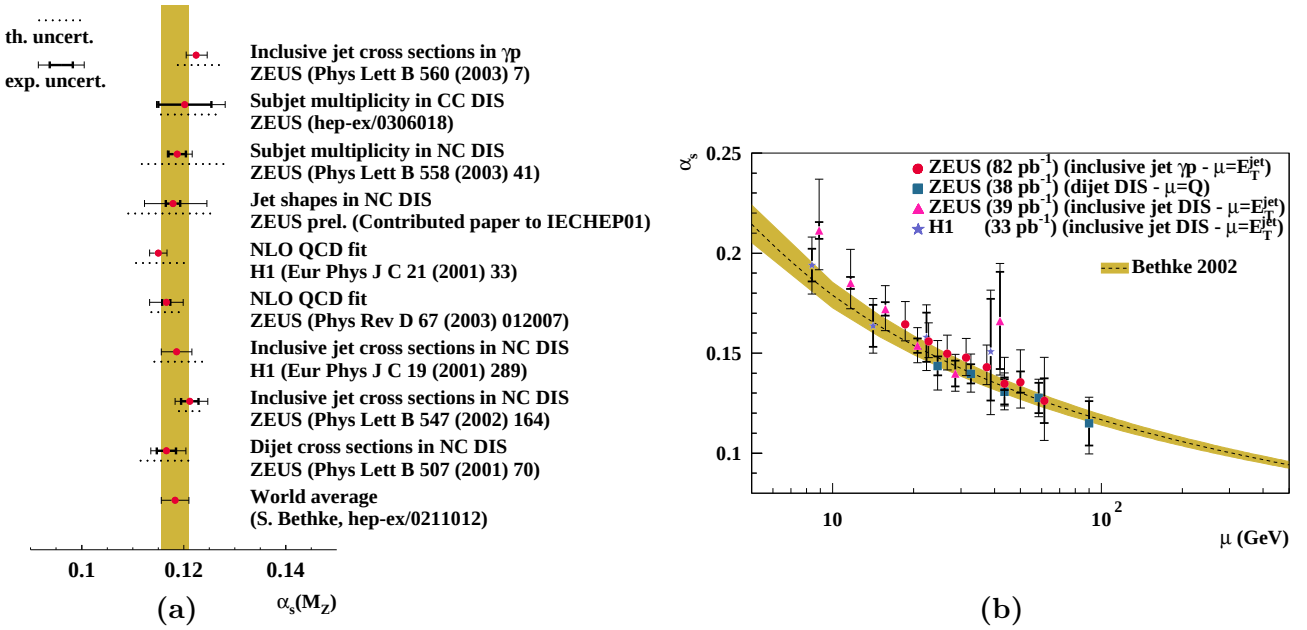

Figure 2: (a) Summary of extracted $\alpha_s(M_Z)$ values at HERA. (b) Summary of extracted $\alpha_s(\mu)$ values as a function of μ at HERA.

BFKL evolution equations; the integration is taken over the full k_T phase space of the gluons with no k_T-ordering.

Another approach, the CCFM evolution equations with angular-ordered parton emission, is equivalent to the BFKL approach for $x \to 0$ and reproduces the DGLAP evolution equations at large x. Thus, the properties of the dijet system, which depend on the dynamics of the ladder, can be studied to determine whether the cascade has a k_T-ordered or unordered evolution.

Deviations from the DGLAP approach at small x can be tested experimentally. At small x it is expected that parton emission along the exchanged gluon ladder should increase with decreasing x. A clear experimental signature of this effect would be that the two outgoing hard partons are no longer back-to-back and so an excess of events at small azimuthal separations should be observed.

Values of the azimuthal separation of the two hard jets in the $\gamma^* p$ centre-of-mass frame, $\Delta\phi^*$, different than π can occur in the DGLAP approach only when higher order contributions are included. On the other hand, in the BFKL and CCFM approaches, the number of events with $\Delta\phi^* < \pi$ should increase due to the partons entering the hard process with large k_T.

3.1 Azimuthal jet separation

To test the predictions of the different approaches, dijet cross sections have been measured [2] using the k_T-cluster algorithm in the longitudinally inclusive mode in the $\gamma^* p$ centre-of-mass frame. The measurements were made in the kinematic region given by $5 < Q^2 < 100$ GeV^2 and $10^{-4} < x < 10^{-2}$. The cross sections refer to jets of $E_T^* > 5$ GeV, $-1 < \eta^{\rm jet}_{\rm LAB} < 2.5$ and $E^*_{T,\rm max} > 7$ GeV, where E_T^* is the jet transverse energy in the $\gamma^* p$ centre-of-mass frame.

Figure 3a shows the measured dijet distribution as a function of $\Delta\phi^*$. A significant fraction of events is observed at a small azimuthal separation. Since a measurement of a multi-differential cross section as a function of x, Q^2 and $\Delta\phi^*$ would be very difficult due to large migrations, the fraction of the number of dijet events with an azimuthal separation between 0 and α, where α

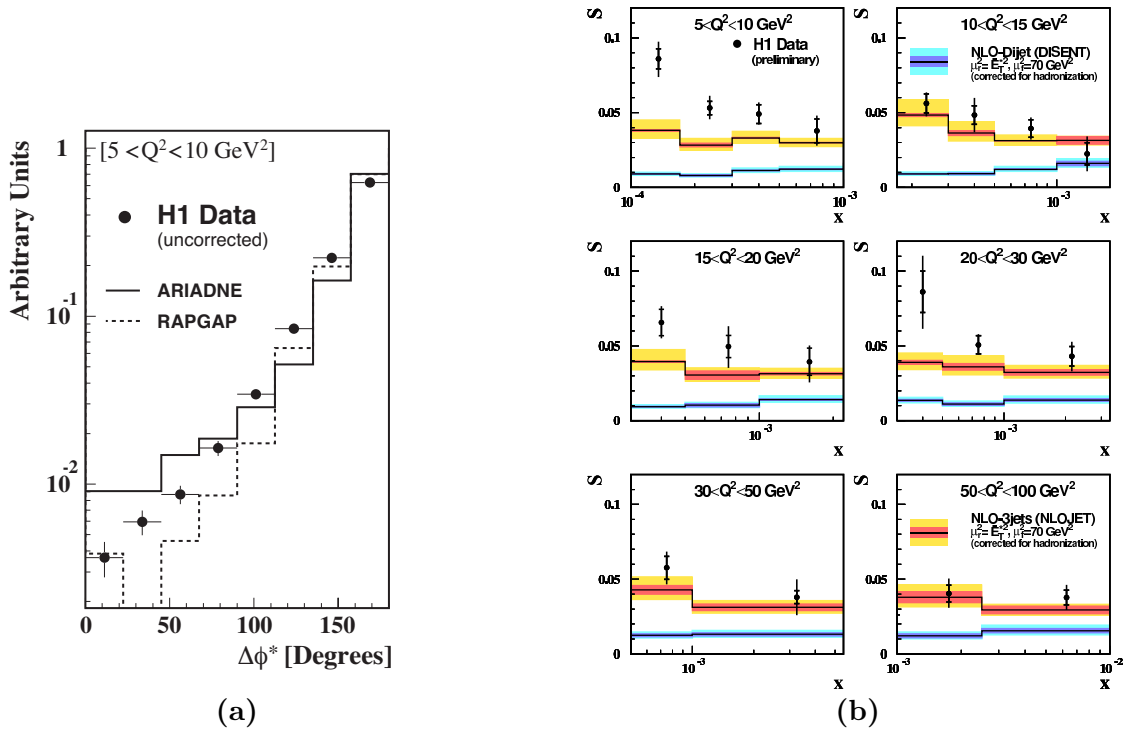

Figure 3: (a) Azimuthal separation between jets [2]. (b) Ratio S as a function of Bjorken x and Q^2 compared with predictions from NLO QCD calculations [2].

was taken as $\alpha = \frac{2}{3}\pi$, was measured instead. The fraction S, defined as

$$S = \frac{\int_0^{\alpha} N_{2\text{jet}}(\Delta\phi^*, x, Q^2) d\Delta\phi^*}{\int_0^{\pi} N_{2\text{jet}}(\Delta\phi^*, x, Q^2) d\Delta\phi^*},$$

is better suited to test small-x effects than a triple differential cross section.

The measured fraction S as a function of Bjorken x in different regions of Q^2 is presented in figure 3b. The data rise towards low x values, especially at low Q^2. The NLO predictions from DISENT, which contain k_T effects only in the first order corrections, are several standard deviations below the data and show no dependence with x. On the other hand, the predictions of NLOJET, which contain k_T effects at next-to-lowest order, provide an accurate description of the data at large Q^2 and large x. However, they fail to describe the increase of the data towards low x values, especially at low Q^2.

Figure 4a shows the data compared with the predictions of RAPGAP with direct only and resolved plus direct processes. A good description of the data is obtained at large Q^2 and large x. However, there is a failure to describe the strong rise of the data towards low x, especially at low Q^2, even when including a possible contribution from resolved virtual photon processes, though the description in other regions is improved.

If the observed discrepancies are due to the influence of non-ordered parton emissions, models based on the color dipole or the CCFM evolution could provide a better description of the data. Figure 4b shows the data compared with ARIADNE (dotted lines) and two predictions of CASCADE which use different sets of unintegrated parton distributions. These sets differ in the way the small-k_T region is treated: in Jung2003 the full splitting function, i.e. including the non-singular term, is used in contrast to JS2001, for which only the singular term was considered. The predictions of ARIADNE give a good description of the data at low x and

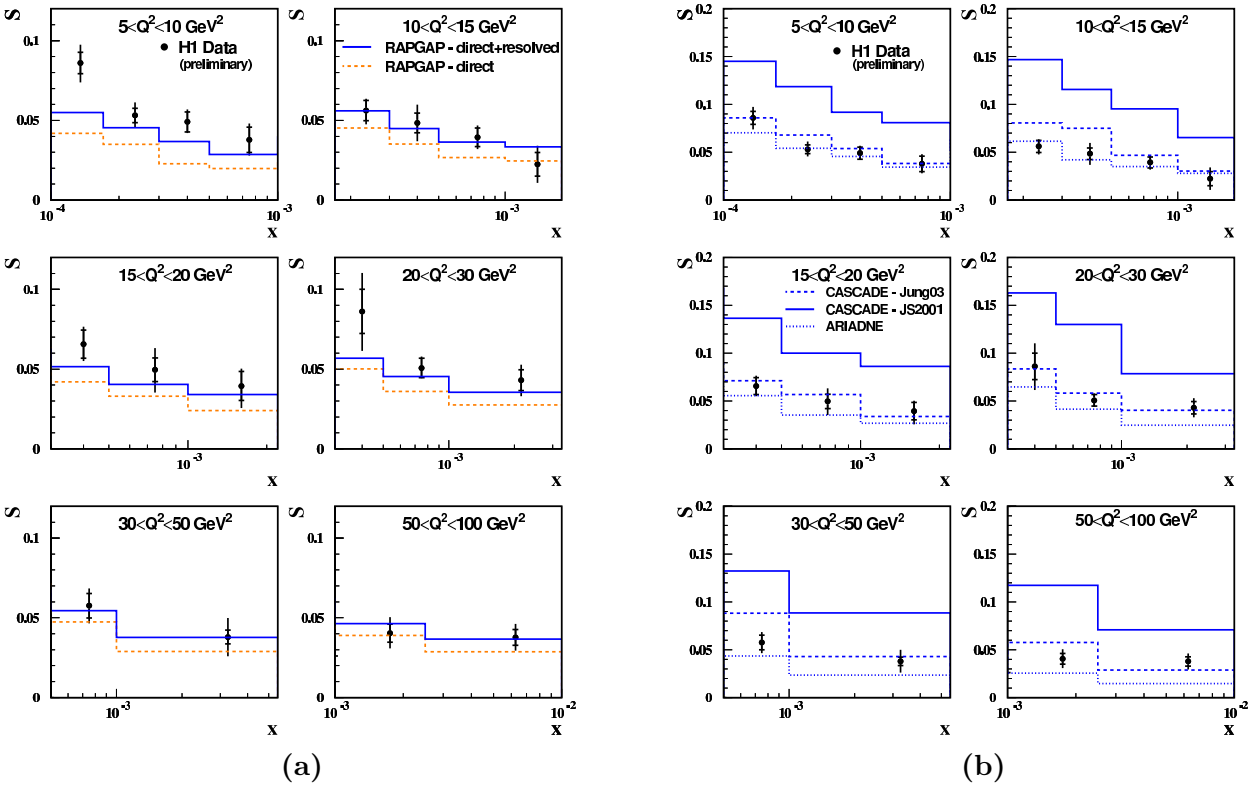

Figure 4: Ratio [2] S as a function of x and Q^2 compared with predictions from RAPGAP (a) and ARIADNE and CASCADE (b).

Q^2, but fail to describe the data at high Q^2. The predictions of CASCADE using JS2001 lie significantly above the data in all x and Q^2 regions, whereas those using Jung2003 are closer to the data. Therefore, the measurement of the fraction S is sensitive to the details of the unintegrated parton distributions.

4 Internal structure of jets

The investigation of the internal structure of jets gives insight into the transition between a parton produced in a hard process and the experimentally observable jet of hadrons. The internal structure of a jet depends mainly on the type of primary parton from which it originated and to a lesser extent on the particular hard scattering process. QCD predicts that at sufficiently high $E_T^{\rm jet}$, where fragmentation effects become negligible, the jet structure is driven by gluon emission off the primary parton and is then calculable in pQCD. The lowest non-trivial order contribution to the jet substructure is given by order $\alpha\alpha_s$ calculations.

The internal structure of the jets can be studied by means of the mean subjet multiplicity. Subjets are resolved within a jet by reapplying the k_T algorithm on all particles belonging to the jet until for every pair of particles the quantity $d_{ij} = \min(E_{T,i}, E_{T,j})^2 \cdot ((\eta_i - \eta_j)^2 + (\varphi_i - \varphi_j)^2)$ is above $d_{\rm cut} = y_{\rm cut} \cdot (E_T^{\rm jet})^2$. All remaining clusters are called subjets. The subjet structure depends upon the value chosen for the resolution parameter $y_{\rm cut}$.

The mean subjet multiplicity has been measured [3] for jets using the k_T algorithm in the HERA laboratory frame with $E_T^{\rm jet}$ above 15 GeV and $-1 < \eta^{\rm jet} < 2$, in the kinematic range given by $Q^2 > 125$ GeV^2. Figure 5a shows the mean subjet multiplicity for a fixed

value of $y_{\rm cut}$ of 10^{-2} as a function of $E_T^{\rm jet}$. It decreases as $E_T^{\rm jet}$ increases, i.e. the jets become more collimated. The experimental uncertainties are small (fragmentation model uncertainty $< 1\%$, the uncertainty on the absolute energy scale of the jets is negligible). The detector and hadronisation corrections are $< 10\%$ and $< 17\%$, respectively, for $E_T^{\rm jet} > 25$ GeV. The data are compared to the LO and NLO predictions of DISENT. The LO calculation fails to describe the data, whereas the NLO calculations provide a good description. These measurements are sensitive to α_s and have been used to extract a value of $\alpha_s(M_Z)$. The result is

$$\alpha_s(M_Z) = 0.1187 \pm 0.0017\ (\text{stat.})\ ^{+0.0024}_{-0.0009}\ (\text{exp.})\ ^{+0.0093}_{-0.0076}\ (\text{th.}).$$

This value is compatible with the world average and with previous measurements (see figure 2a).

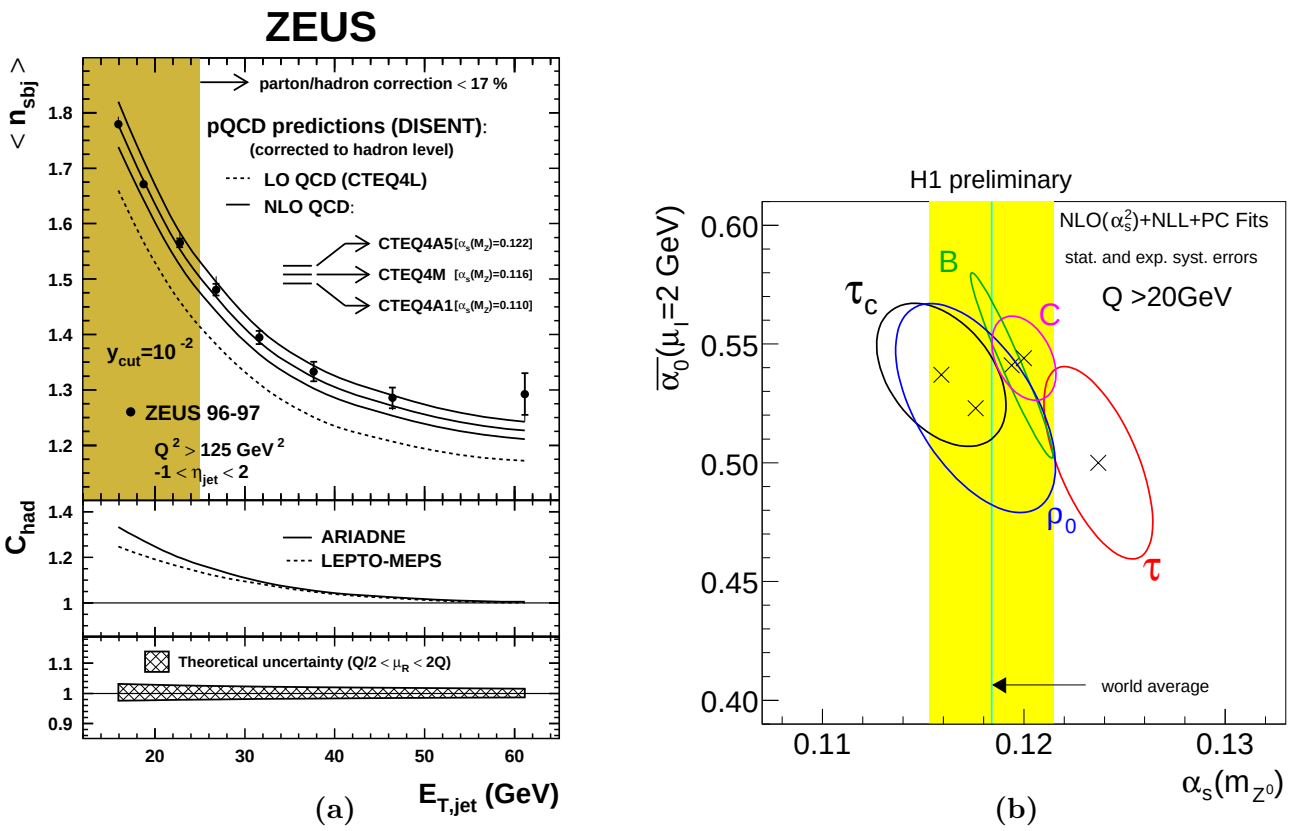

Figure 5: (a) Mean subjet multiplicity [1] as a function of $E_T^{\rm jet}$. (b) $1-\sigma$ contours in the $(\alpha_s, \bar{\alpha}_0)$ plane [4].

5 Event shapes

A complementary extraction of α_s, also using the details of the hadronic final state in DIS, comes from the study of the event shape variables, like thrust or jet broadening. Event shape variables are particularly sensitive to the details of the non-perturbative effects of hadronisation and can be used to test the models for these effects. Recently, new developments with regard to power-law corrections have prompted a revived interest in the understanding of hadronisation from first principles. In this type of analysis, the data are compared to model predictions which combine NLO calculations and the theoretical expectations of the power corrections, which are characterised by an effective coupling $\bar{\alpha}_0$. Previous results supported the concept of power

corrections in the approach of Dokshitzer et al. but a large spread of the results suggested that higher order corrections were needed. Now, resummed NLL calculations matched to NLO are available and so it is possible to study event shape distributions instead of only their mean values.

Event shape distributions (thrust, jet broadening, the jet mass ρ and the C parameter) have been measured [4] for particles in the current hemisphere in the kinematic region given by $14 < Q < 200$ GeV and $0.1 < y < 0.7$, where y is the inelasticity variable. Predictions consisting of NLO calculations using DISASTER++, resummed calculations matched to NLO and power corrections have been fitted to the data, leaving α_s and $\bar{\alpha}_0$ as free parameters. A good description of the data by the predictions was obtained at high Q^2, though the description at low Q^2 was poorer. Figure 5b shows the 1σ-contour results from the fit in the α_s-$\bar{\alpha}_0$ plane. The spread observed in previous studies is much reduced when the resummed calculations are included. A clear anti-correlation between α_s and $\bar{\alpha}_0$ is found for all variables. A universal value for $\bar{\alpha}_0$ of 0.5 at the 10% level was obtained, in agreement with the previous results, but with a smaller spread. There is still a sizeable theoretical uncertainty for both α_s and $\bar{\alpha}_0$, of the order of 5%, which is as large as the experimental uncertainties. This uncertainty comes from the absent higher order corrections.

6 Conclusions

HERA has become a unique QCD-testing machine due to the fact that at large scales considerable progress in understanding and reducing the experimental and theoretical uncertainties has led to very precise measurements of the fundamental parameter of the theory, the strong coupling constant α_s. The use of observables resulting from jet algorithms leads now to determinations that are as precise as those coming from more inclusive measurements, such as from τ decays. To obtain even better accuracy in the determination of QCD, further improvements in the QCD calculations are needed, e.g. next-to-next-to-leading-order corrections.

At low values of x and Q^2, considerable progress has also been obtained in understanding the mechanisms of parton emission, though the interplay between the DGLAP, BFKL and CCFM evolution schemes has still to be fully worked out. Further progress in this respect needs both more experimental and more theoretical work.

Acknowledgments

I would like to thank the organisers for providing a warm atmosphere conducive to many physics discussions and a well organised conference. Special thanks to my colleagues from H1 and ZEUS for their help in preparing this report.

References

[1] ZEUS Collaboration, S. Chekanov et al., *Phys. Lett.* **B547**, 164 (2002).

[2] H1 Collaboration, Contributed paper N81 to the International Europhysics Conference on High Energy Physics, July 17-23,2003, Aachen.

[3] ZEUS Collaboration, S. Chekanov et al., *Phys. Lett.* **B558**, 41 (2003).

[4] H1 Collaboration, Contributed paper N111 to the International Europhysics Conference on High Energy Physics, July 17-23,2003, Aachen.